ELSEVIER

Journal of Organometallic Chemistry 578 (1999) 155–168

Journal of Organometallic Chemistry

Reactions of $M(C{\equiv}CC{\equiv}CR)(CO)_3Cp$ [M = Mo, W; R = H, $Fe(CO)_2Cp$, $M(CO)_3Cp$] with cobalt carbonyls: X-ray structures of $\{Cp(OC)_8Co_2M(\mu_3\text{-}C)\}C{\equiv}C\{(\mu_3\text{-}C)Co_2M'(CO)_8Cp\}$ (M = M′ = Mo, W; M = Mo, M′ = W)

Michael I. Bruce [a,*], Jean-François Halet [b,1], Samia Kahlal [b], Paul J. Low [a], Brian W. Skelton [c], Allan H. White [c]

[a] *Department of Chemistry, University of Adelaide, Adelaide, South Australia 5005, Australia*
[b] *Laboratoire de Chimie du Solide et Inorganique Moléculaire, UMR CNRS 6511, Université de Rennes 1, 35042 Rennes Cedex, France*
[c] *Department of Chemistry, University of Western Australia, Nedlands, Western Australia 6907, Australia*

Received 6 August 1998

Abstract

Reactions of $Co_2(CO)_8$ with complexes $M(C{\equiv}CC{\equiv}CR)(CO)_3Cp$ [M = Mo, W; R = H, $Fe(CO)_2Cp$] are described. Simple adducts containing a $Co_2(CO)_6$ group attached to the least sterically-hindered C≡C triple bond are formed. In contrast, when R = $M(CO)_3Cp$ (M = Mo, W), bis-cluster complexes $\{Cp(OC)_8Co_2M(\mu_3\text{-}C)\}C{\equiv}C\{(\mu_3\text{-}C)Co_2M'(CO)_8Cp\}$ (M = M′ = Mo, W; M = Mo, M′ = W) were obtained. All three complexes were structurally characterised. Important features are the presence of both *distal* and *proximal* Cp groups in each molecule, and the formal oxidation of the –C≡C–C≡C– chain in the precursor to ≡C–C≡C–C≡ system in the products. Extended Hückel and Density Functional Theory calculations have been used to rationalise the observed structures of the $M_3C_4M_3$ complexes. The reaction between $Co_2(\mu\text{-dppm})(CO)_6$ and $\{W(CO)_3Cp\}_2(\mu\text{-}C_4)$ gave the simple adduct $Co_2(\mu\text{-dppm})\{\mu\text{-}[Cp(OC)_3W]C_2C{\equiv}C[W(CO)_3Cp]\}(CO)_4$.

Keywords: Alkyne; Carbon chain; Carbyne; Cluster; Cobalt; Tungsten

1. Introduction

The current intense interest in complexes containing all-carbon ligands is manifested in the appearance of the present volume. Our own studies have recently concentrated on the C_4 molecule and an extensive chemistry of its derivatives including compounds containing C_4 chains capped at each end by the same or different ML_n groups is being developed rapidly by several groups [1–6]. The number of metal cluster complexes containing the C_4 ligand is much smaller, to our present knowledge reported examples being limited to $[\{Fe_3(CO)_9\}_2(\mu_3{:}\mu_3\text{-}C_4)]^{2-}$ (**1**) [7], $\{Co_3(CO)_9\}_2(\mu_3{:}\mu_3\text{-}C_4)$ (**2**) [8] and its $P(OR)_3$ (R = Me, Ph) derivatives [9], $\{Ru_3(\mu\text{-}PPh_2)(CO)_9\}_2(\mu_3{:}\mu_3\text{-}C_4)$ (**3**) [10], $Ru_3(\mu\text{-H})\{\mu_3\text{-}C_4[W(CO)_3Cp]\}(CO)_9$ (**4**) [11] and $Os_3(\mu\text{-H})\{\mu_{2+n}\text{-}C_4[Re(NO)(PPh_3)Cp^*]\}(CO)_{10-n}$ ($n = 0, 1$) [12].

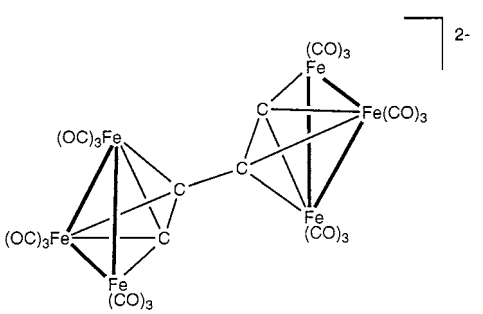

(1)

* Corresponding author. Fax: +61-8-83034358.
E-mail addresses: mbruce@chemistry.adelaide.edu.au (M.I. Bruce), jean-francois.halet@univ-rennes1.fr (J.-F. Halet)
[1] Also corresponding author. Fax: +33-2-99383487.

0022-328X/99/$ - see front matter
PII: S0022-328X(98)01118-8

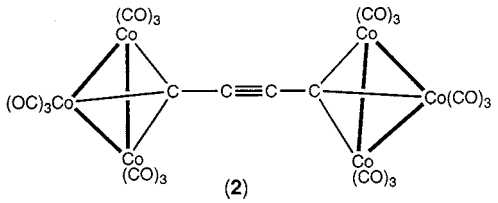

(2)

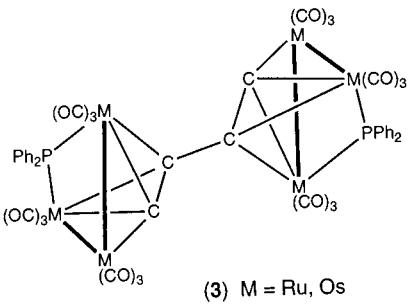

(3) M = Ru, Os

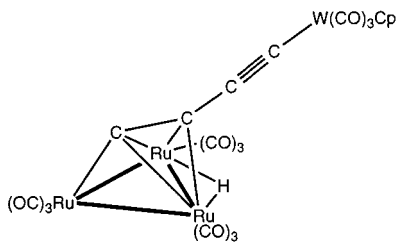

(4)

Related complexes containing C_4 ligands bridging two $M_2(\mu\text{-}PPh_2)(CO)_6$ (M = Fe [13], Ru [14]) groups have also been described. In the course of studies of the reactivity of complexes of the type $M(C{\equiv}CC{\equiv}CR)(CO)_3Cp$ (M = Mo, W; R = H or other metal–ligand combination) [15–17], we have examined the reactions of some of these complexes with the cobalt carbonyls $Co_2(CO)_8$ and $Co_2(\mu\text{-dppm})(CO)_6$; below we describe the novel products obtained therefrom.

2. Results and discussion

Dicobalt octacarbonyl, $Co_2(CO)_8$, is known to react with a number of organometallic acetylides $M(C{\equiv}CR)(L)_n$ to give simple adducts, $Co_2\{\mu\text{-}\eta^2\text{-}RC_2[ML_n]\}(CO)_6$ (e.g. R = Me, Ph; ML_n = $Mn(CO)_4(PCy_3)$ [18], $Fe(CO)_2Cp$ [19–21], $Ru(CO)_2Cp$ [21]). In other cases, trinuclear compounds of general form $Co_2M(\mu_3\text{-}\eta^2\text{-}C_2R')(CO)_6(L)_n$ are formed directly, presumably via intermediate adducts [19]. Oxidative decarbonation of $Co_2\{\mu\text{-}PhC_2[M(CO)_2Cp]\}(CO)_6$ (M = Fe, Ru) affords the benzylidyne clusters $Co_2M(\mu_3\text{-}CPh)(CO)_8Cp$ [21]. Coordination of $Co_2(CO)_6$ moieties to each C≡C triple bond of organic diacetylenes has also been reported [22–25]. We were therefore interested to examine the reactions of several $M(C{\equiv}CC{\equiv}CR)(CO)_3Cp$ complexes [M = W, Mo; R = H, $Fe(CO)_2Cp$, $M(CO)_3Cp$] with $Co_2(CO)_8$ both to probe the reactivity of the C≡C triple bonds and to investigate the possibility of forming new cluster compounds.

The reactions of $Co_2(CO)_8$ with the diynyl complexes $M(C{\equiv}CC{\equiv}CH)(CO)_3Cp$ (M = W **5-W**; Mo **5-Mo**) gave the expected adducts $Co_2\{\mu\text{-}HC_2C{\equiv}C[M(CO)_3Cp]\}(CO)_6$ (M = W **6-W**; Mo **6-Mo**) as dark red crystalline materials. The complexes were characterised by the usual spectroscopic and microanalytical methods. The IR spectra of these adducts in the ν(CO) region approximated to a superposition of the usual $M(CO)_3Cp$ and $Co_2(\mu\text{-}RC_2R')(CO)_6$ patterns. Low field singlet resonances in their ^{1}H-NMR spectra at δ 6.04 (**6-W**) and 6.06 (**6-Mo**) are assigned to the ≡CH protons and are considerably shifted downfield from the resonances at δ 2.03 and 2.04 found in **5-W** and **5-Mo**, respectively [17], suggesting that coordination of the cobalt fragment had occured at the least sterically hindered C≡C triple bond. The four carbons of the C_4 chain appeared as singlets at δ 123.13, 94.34, 73.84 and 71.56 (for **6-W**) and at δ 123.93, 109.52, 74.07 and 71.35 (for **6-Mo**). These values may be compared with those found for **5-W** (δ 110.32, 72.77, 70.87, 66.07) [17] and surprisingly do not offer such unequivocal evidence for the site of coordination.

These reactions with the diynyl complexes **5-W** and **5-Mo** thus proceeded as expected to give **6-W** and **6-Mo** respectively in which a $Co_2(CO)_6$ fragment has coordinated to the C≡C moiety adjacent to the diynyl proton (Scheme 1). This result is by no means surprising. The approach of the cobalt reagent to the C≡C adjacent to the metal centre is hindered to some degree by the cyclopentadienyl and carbonyl ligands, and we consider this to be the most significant factor in determining the site of coordination. However, since the μ-alkyne ligands in $Co_2(\mu\text{-}RC_2R')(CO)_6$ complexes are displaced at ambient temperature by alkynes with more electronegative substituents [26], it should be noted that the different electronic natures of the $M(CO)_3Cp$ and H end-caps may also be a factor.

The mixed metal diyndiyl complex $\{Cp(OC)_2Fe\}C{\equiv}CC{\equiv}C\{W(CO)_3Cp\}$ (**7**) also reacted smoothly with $Co_2(CO)_8$ to give the similar adduct $Co_2\{\mu\text{-}[Cp(OC)_2Fe]C_2C{\equiv}C[W(CO)_3Cp]\}(CO)_6$ (**8**) after reaction with $Co_2(CO)_8$. There was no evidence for the formation of any other product. Coordination of the di-cobalt moiety to the C≡C triple bond adjacent to the less sterically demanding $Fe(CO)_2Cp$ fragment was established from trends observed when the NMR spectra of **7** and **8** were compared. The distinct cyclopentadienyl ligands of the precursor **7** gave rise to two sets of singlet resonances in the ^{1}H- (δ 5.62 (W) and 5.03 (Fe)) and ^{13}C- (δ 91.56 (W) and 85.28 (Fe)) NMR spectra

[16]. Analogous signals in the cobalt adduct **8** were observed at δ 5.67 (W) and 5.16 (Fe) and δ 91.85 (W) and 86.68 (Fe). It would therefore appear that a greater change in environment had occurred near the Fe centre. Changes in the ^{13}C-NMR spectra were not helpful in this regard. For **8**, the four C(sp) resonances are found at δ 125.79, 106.09, 97.86 and 85.68 which, when compared with values of δ 115.45, 101.00, 63.32 and 42.32 found for precursor **7**, and those of **6-W**, are consistent with the proposed structure. It is evident that further studies of the spectra of these and related complexes are necessary before definitive assignments can be made.

Attempts to form tetra-cobalt complexes of general form $\{Co_2(CO)_6\}_2\{\mu\text{-}\eta^2;\mu\text{-}\eta^2\text{-}[Cp(CO)_3M]C_2C_2R\}$ [R = H, M = Mo, W; R = $Fe(CO)_2Cp$] by reactions of **5**, **6**, **7** or **8** with an excess of $Co_2(CO)_8$ were unsuccessful, and only complexes **6** or **8** were isolated in yields essentially identical to those from the stoichiometric reactions. In this case the selectivity of the reaction is difficult to resolve using an electronic argument, and we favour an explanation based upon the increased steric hindrance about the C_2 unit adjacent to the $W(CO)_3Cp$ group. The carbonyl ligands in $Fe(C{\equiv}CR)(CO)_2Cp$ complexes are bent back from from the acetylide substituent to a greater extent than the equivalent carbonyl ligands in $W(C{\equiv}CR)(CO)_3Cp$ complexes. This results in the C_2 moiety adjacent to the iron centre being more accessible to the cobalt carbonyl reagent. Similarly, hindered alkynes are also inert to reactions with $Co_2(CO)_8$ [26].

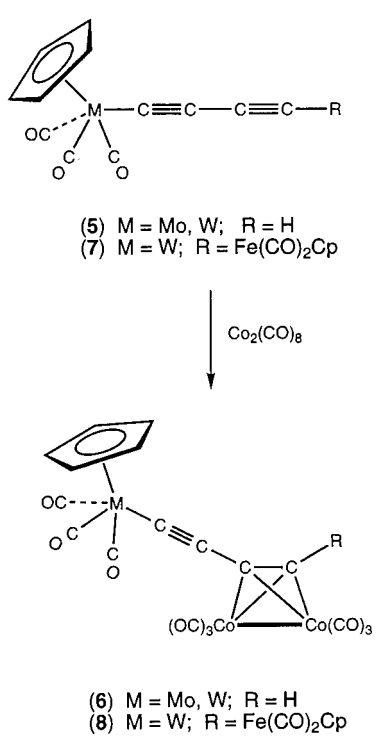

Scheme 1.

In contrast to these results, reactions of $Co_2(CO)_8$ with the diyndiyl complexes $\{Cp(OC)_3M\}C{\equiv}CC{\equiv}C\{M'(CO)_3Cp\}$ (M = M′ = W **9-W**, Mo **9-Mo**; M = W, M′ = Mo **10**), in which both ends of the C_4 chain are terminated by bulky $M(CO)_3Cp$ groups, gave the dark red products in yields of between 20 and 40%. The IR spectra in the ν(CO) region were more complex than expected for the simple dicobalt hexacarbonyl adducts $Co_2\{\mu\text{-}[Cp(OC)_3M]C_2C{\equiv}C[M(CO)_3Cp]\}(CO)_6$ and included weak broad bands at ca. 1890 cm^{-1} which suggested the presence of bridging carbonyl ligand(s). Their molecular structures were established as the cluster-capped ethynes $\{Cp(OC)_8Co_2M(\mu_3\text{-}C)\}C{\equiv}C\{(\mu_3\text{-}C)Co_2M'(CO)_8Cp\}$ (M = M′ = W **11-W**, Mo **11-Mo**; M = W, M′ = Mo **12**) from single-crystal X-ray determinations in each case (vide infra).

In the ^{1}H- and ^{13}C-NMR spectra of **11-W** and **11-Mo**, only singlet resonances were observed for the Cp ligands at δ 5.56 and 5.49, respectively. By comparison, the two signals at δ 5.57 and 5.49 found for **12** can be assigned to the Cp(W) and Cp(Mo) groups, respectively. Similarly, the ^{13}C-NMR spectra contained singlet Cp resonances at δ 91.32 (**11-W**), 93.45 (**11-Mo**), and at 91.21 and 93.56 [**12**; Cp(W) and Cp(Mo), respectively]. The C≡C and CO resonances were found at δ 126.48 and 202.96 (**11-W**), 125.94 and 207.90 (**11-Mo**) while for the mixed W/Mo complex **12**, two sets of signals were observed for these ligands (C≡C at δ 127.65, 124.76; CO at 202.85, 207.92) on the W and Mo clusters, respectively. Only in the case of **11-Mo** was the μ_3-C signal detected, at δ 269.85. The negative-ion electrospray mass spectra (ES-MS) spectra were obtained in the presence of NaOMe and contained ions at m/z 1259 (**11-W**), 1084 (**11-Mo**) and 1173 (**12**), assigned to $[M + OMe]^-$.

Only **11** or **12** could be isolated along with the unreacted diyndiyl reagent by slow addition of $Co_2(CO)_8$ to an excess of **9** or **10**, the simple adducts $Co_2\{\mu\text{-}[Cp(OC)_3M]C_2C{\equiv}C[M(CO)_3Cp]\}(CO)_6$ (M = W, Mo) not being detected. The formation of these products may be considered as proceeding via addition of a $Co_2(CO)_6$ fragment to one or both of the C≡C triple bonds in **9** or **10** to give the undetected intermediates such as $\{Co_2(CO)_6\}_2\{\mu,\eta^2\text{:}\mu,\eta^2\text{-}[Cp(OC)_3M]C_2C_2[M(CO)_3Cp]\}(CO)_6$ (Scheme 2). Loss of CO induced by steric congestion results in formation of new metal–metal bonds and with a consequent redistribution of electron denisty through the C_4 bridge. The electronic reorganisation is a formal oxidation of the C_4 ligand and is similar to the processes occurring on oxidation of dinuclear complexes containing this ligand, such as $\{Ru(PPh_3)_2Cp\}_2(\mu\text{-}C_4)$ [27]. In turn, this leads to displacement of a CO ligand from the second Group 6 centre, followed by addition of $Co_2(CO)_6$ to the resulting M≡C fragment to give the products **11** and

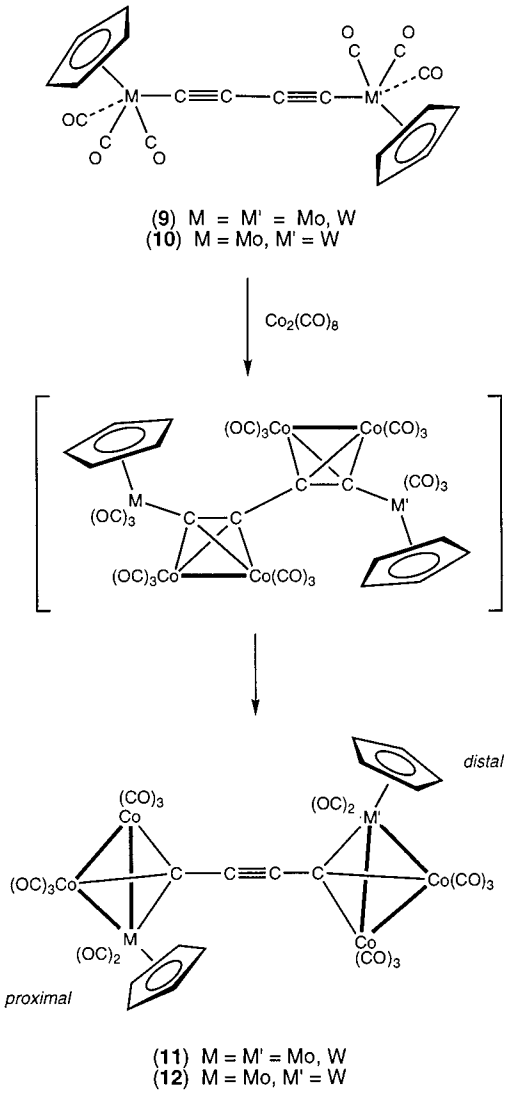

(11) M = M' = Mo, W
(12) M = Mo, M' = W

Scheme 2.

12, in a process reminiscent of the extensive reactions of $W(\equiv CC_6H_4Me4)(CO)_2Cp$ with a variety of metal substrates [28].

*2.1. Molecular structures of $\{Cp(OC)_8Co_2M(\mu_3\text{-}C)\}C\equiv C\{(\mu_3\text{-}C)Co_2M'(CO)_8Cp\}$ [M = M′ = W (**11-W**), Mo (**11-Mo**); M = W, M′ = Mo (**12**)]*

A plot of a single molecule of **11-Mo**, as typical of the three isomorphous complexes, is given in Fig. 1 and significant structural parameters for all three complexes are collected in Table 1. All are isostructural and contain two triangular Co_2M clusters, one at each end of the C_4 chain. In **12**, a 50:50 disorder of Mo and W atoms renders the two Co_2M clusters similar. The M atoms have a Cp and two CO ligands, while the Co atoms bear three CO ligands. The structures are similar to that of the previously described complex $\{Co_3(CO)_9(\mu_3\text{-}C)\}_2C_2$ (**2**), which was one of the products obtained by dehalogenation of $Co_3(\mu_3\text{-}CX)(CO)_9$ (X = Cl, Br) [8]. There are also many examples of heterometallic $Co_2M(\mu_3\text{-}CR)$ clusters to which the end capping clusters in **11** and **12** may be compared [29].

Of most interest in the present context is the geometry of the C_4 chain. Along the chain, the three C–C distances are 1.385(6)–1.39(1), 1.19(1)–1.216(8) and 1.380(8)–1.40(1) Å, i.e. a long-short-long arrangement, consistent with disubstituted ethyne formulation given above. The C(1)-C(2) separations are somewhat shorter than the C(carbyne)–C(*ipso*) bond lengths in $Co_2Mo(\mu_3\text{-}CPh)(CO)_8Cp$ (1.49(1) Å) [30] and $Co_2W\{\mu_3\text{-}C(C_6H_4Me\text{-}4)\}(CO)_8Cp$ (1.496(10) Å) [31] or the C–CO_2Pr^i separation in $Co_2M\{\mu_3\text{-}C(CO_2Pr^i)\}(CO)_8Cp^*$ (1.459(9) Å) [32]. The central C(2)–C(3) bond is shorter than the similar bond in **2** [1.241(2) Å] [8]. This arrangement contrasts sharply with that found in the precursors **9** and **10**, which on spectroscopic grounds are formulated as being diyndiyl derivatives with a short-long-short sequence of C–C bonds along the chain.

The two Co_2M clusters are not identical, however. The Cp ligand in one (moiety '1') is *proximal* to the C_4 chain, lying above the M(11)–C(1) vector, while in the other (moiety '2'), the Cp group is *distal* to the C_4 chain, being approximately *trans* to the M(21)–C(4) vector. This difference in geometry results in the MCo_2 triangles being approximately staggered about the C_4 ligand, as was found in **2**. In the *proximal* component, the CO ligands associated with the Group 6 metal atom are found to be semi-bridging, and characteristic ν(CO) bands associated with this motif are observed in the infrared spectra. The structural parameters are also significantly different in the two clusters. The metal–metal bonds are shorter in the Co_2M_{distal} clusters than in the $Co_2M_{proximal}$ clusters, the ranges being 2.497(3)–2.499(1) versus 2.510(1)–2.518(2) (Co–Co), 2.663(1)–2.698(1) versus 2.723(1)–2.7674(7) Å (Co–M) [the similar atomic radii of Mo and W result in there being no significant differences between the Co–Mo and Co–W separations]. In **12**, it may be noted that both Co_2M triangles are unsymmetrical, and that the cluster bearing the *proximal* Cp ligand is expanded overall with respect to the *distal* moiety. There is also some asymmetry in the two M–Co distances, e.g. for the cluster moiety '1', values of 2.723(1)–2.726(2) and 2.7642(9)–2.7674(4) Å are found, compared with 2.663(1)–2.6708(6) and 2.688(2)–2.698(1) Å for cluster moiety '2'. The metal–carbon separations show a similar but less pronounced trend in the M–C distances (2.05(1)–2.076(5) versus 2.096(9)–2.107(4) Å); differences in the Co–C distances are not significant.

Several detailed studies of the geometries of complexes $Co_2M(\mu_3\text{-}CR)(CO)_8Cp'$ (M = Mo, W; R = aryl,

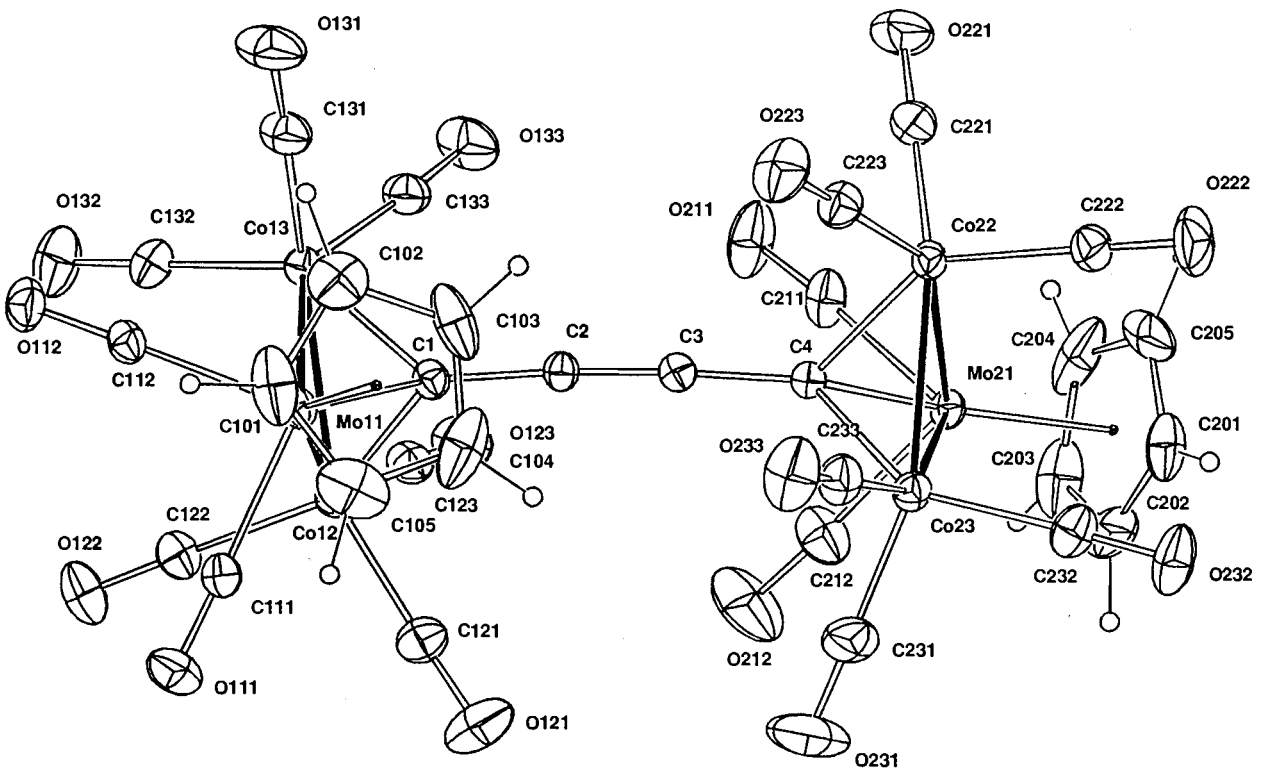

Fig. 1. Plot of a molecule of $\{Co_2Mo(CO)_8Cp\}_2(\mu_3{:}\mu_3\text{-}C_4)$ (**11-Mo**), showing the atom numbering scheme. Non-hydrogen atoms are shown with 20% thermal envelopes; hydrogen atoms have arbitrary radii of 0.1 Å.

alkyl, CO_2R'; $Cp' = C_5H_5$, C_5H_4Me, C_5Me_5) have been made, both in both solution and in the solid state [30–34]. Two distinct isomers have been identified, which are distinguished by the orientation of the Cp′ ring relative to the μ_3-CR capping ligand, as found above. For $Cp' = \eta^5\text{-}C_5H_5$ or $\eta^5\text{-}C_5H_4Me$ [30,31] the Cp′ ring is located in the *distal* position, while for $Cp' = \eta^5\text{-}C_5Me_5$, the Cp′ group is *proximal* [32]. In the solid-state structures of the *proximal* isomers, the CO ligands bound to the Group 6 metal atom are semi-bridging the Co–M vectors and characteristic low-energy ν(CO) bands associated with this motif are found in their IR spectra. It has been suggested that one of the principal factors determining the geometrical arrangement of these clusters is the electronic nature of the Cp′ ligand, *proximal* orientation of the $M(CO)_2Cp'$ fragment leading to improved electron donation to the other two metal centres and the carbyne carbon. As has been found in the related $Co_2M(\mu_3\text{-}CR)(CO)_8Cp'$ ($Cp' = \eta^5\text{-}C_5H_5$ and $\eta^5\text{-}C_5H_4Me$) compounds mentioned above, complexes **11** and **12** are fluxional in solution at room temperature and the *proximal* and *distal* isomers are not individually detected. Thus, only single resonances are observed in the ^{13}C-NMR spectra for the CO (broad), Cp and carbyne carbons. In the case of **12**, however, the ligands associated with the Co_2Mo cluster moiety may be distinguished from those of the Co_2W cluster.

2.2. Electron distribution in $\{Cp(OC)_8Co_2M(\mu_3\text{-}C)\}_2C_2$ complexes

As mentioned earlier, cluster species **11** and **12** are closely related to the cobalt cluster $\{(CO)_9Co_3(\mu_3\text{-}C)\}(\mu\text{-}C{\equiv}C)\{(\mu_3\text{-}C)Co_3(CO)_9\}$ (**2**) [8] and its phosphine and phosphite derivatives [9]. Considering formally the C_4 ligand as neutral, that is acting as a six-electron donor to the metallic $Co_6(CO)_{18}$ fragment, a metallic valence electron (MVE) count of 96 (9 [Co] × 6 + 2 [CO] × 18 + 6 [C_4] = 96) is obtained for **2**. Such an electron count is predicted by the Polyhedral Skeletal Electron Pair (PSEP) rule [35] for this complex made of two 48-MVE triangular moieties linked through the C_4 unit. The application of the Effective Atomic Number (EAN) formalism also leads to this electron count. Compound **2** is an electron-precise molecule. If electrons of the C_4 unit not involved in the M–C bonding are added, a total cluster-valence-electron (CVE) count of 106 is achieved. Such a CVE count renders **2** isoelectronic (but not isostructural) with $\{Ru_3(\mu\text{-}PPh_2)(CO)_9\}_2(\mu_3{:}\mu_3\text{-}C_4)$ (**3**), the M_6C_4 core of which consists of two open M_3 triangles bridged by a bent C_4 fragment [10].

In order to clarify the electronic structure of such M_6C_4 compounds, in particular to see whether intracluster interaction occurs between the metallic cores through the unsaturated carbon bridge, Extended

Table 1
Selected geometries in **11-Mo**, **W** and **12**[a]

Complex/metal	**11-Mo**/Mo	**11-W**/W	**12**/Mo/W
(a) Cluster fragment bond length (Å)			
Co(*n*2)–Co(*n*3)	2.5109(9)	2.518(2)	2.510(1)
	2.498(1)	*2.497(3)*	*2.499(1)*
M(*n*1)–Co(*n*2)	2.7674(7)	2.767(1)	2.7641(9)
	2.6708(6)	*2.663(1)*	*2.6658(8)*
M(*n*1)–Co(*n*3)	2.7247(9)	2.726(2)	2.723(1)
	2.698(1)	*2.688(2)*	*2.689(1)*
Co(*n*2)–C(α)	1.934(4)	1.967(9)	1.933(5)
	1.932(4)	*1.94(1)*	*1.931(6)*
Co(*n*3)–C(α)	1.950(5)	1.95(1)	1.940(6)
	1.937(4)	*1.95(1)*	*1.938(6)*
M(*n*1)–C(α)	2.076(5)	2.05(1)	2.054(6)
	2.107(4)	*2.096(9)*	*2.104(5)*
Cluster fragment bond angle (°)			
Co(*n*2)–C(α)–C(β)	124.3(2)	122.6(9)	123.2(3)
	128.6(3)	*128.5(6)*	*128.5(3)*
Co(*n*3)–C(α)–C(β)	130.1(4)	130(1)	129.9(6)
	127.1(4)	*127(1)*	*126.4(5)*
M(*n*1)–C(α)–C(β)	132.6(3)	134.0(8)	132.6(4)
	135.6(3)	*136.6(7)*	*136.4(4)*
Cp(*n*00)–M(*n*1)–C(α)	112.4	112.2	112.8
	164.6	164.7	164.9
(b) C_4 ligand bond lengths (Å)			
C(1)–C(2)	1.385(6)	1.39(1)	1.397(8)
C(2)–C(3)	1.216(6)	1.19(1)	1.215(8)
C(3)–C(4)	1.380(6)	1.40(1)	1.386(9)
C_4 ligand bond angle (°)			
C(1)–C(2)–C(3)	175.7(5)	176(1)	176.1(7)
C(2)–C(3)–C(4)	176.9(4)	178(1)	177.0(5)

[a] Values for the '*distal*' moiety ($n = 2$) are given *italicized* below those for the '*proximal*' moiety ($n = 1$).

Hückel Theory (EHT) and Density Functional Theory (DFT) calculations were first carried out on the hexacobalt species **2**. The actual symmetry of **2** is close to D_{3d} [8]. Therefore, compound **2** was optimized with the aid of DFT calculations under the D_{3d} symmetry constraint in order to reduce computational effort. A rather good agreement is observed between the optimized and experimental geometries, in particular the

Table 2
Comparison of computed and experimental bond distances (Å) for compound **2**

	Computed	Experimental[a]
Co–Co	2.485	2.470(10)[b]
Co–C_α	1.907	1.92(1)[b]
Co–C_{eq}(O)	1.745	1.78(2)[b]
Co–C_{ax}(O)	1.747	1.82(1)[b]
C–O	1.16	1.13(1)[b]
C_α–C_β	1.366	1.37(1)
C_α–$C_{\beta'}$	1.238	1.24(2)

[a] See [8].
[b] Averaged.

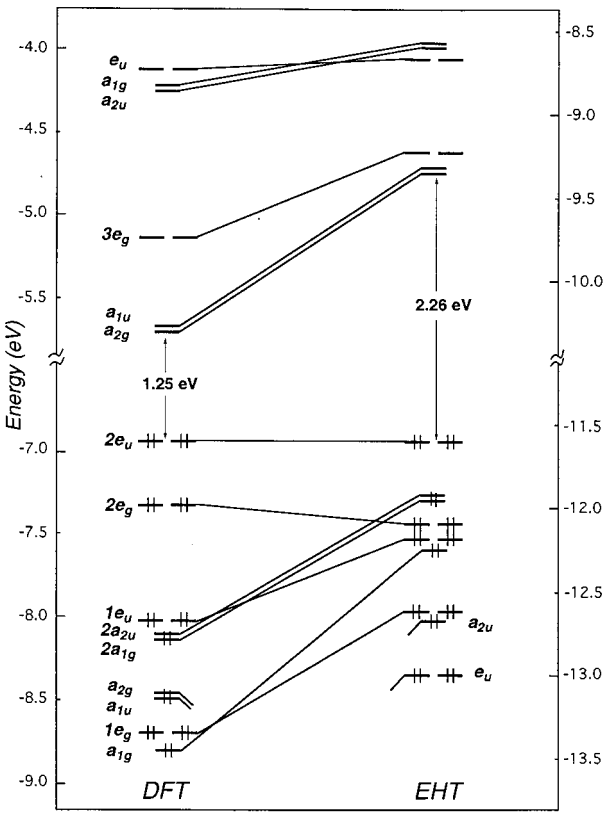

Fig. 2. DFT (left) and EHT (right) MO diagrams for compound **2**.

Co–Co, Co–C_α and C–C separations (see Table 2). The largest deviation concerns the Co–C(O) distances, computed to be 0.04–0.07 Å shorter than the experimental values.

The DFT MO diagram of the optimized geometry of **2** is shown in Fig. 2. A closed-shell electron configuration with a large HOMO–LUMO gap (1.25 eV) is computed for the observed count of 96 MVEs. A comparable MO diagram is obtained with EHT calculations (see Fig. 2). The same closed-shell electron configuration is obtained, with a somewhat larger HOMO–LUMO gap of 2.26 eV. The composition of the MOs in the HOMO–LUMO region is similar for both DFT and EHT results. Therefore, because of their structural complexity (size of the molecule, low symmetry) the detailed analyses of the bonding in **2** and related species **11** was carried out using EHT calculations.

The qualitative MO diagram of the hexacobalt cluster **2** is shown in Fig. 3, based on the interaction of the frontier molecular orbitals (FMOs) of the $\{(CO)_9Co_3\cdots Co_3(CO)_9\}$ fragment with the FMOs of the C_4 unit. The fragments are arbitrarily considered as neutral.

The metallic fragment consists of two non-interacting $Co_3(CO)_9$ units. The FMOs of a $Co_3(CO)_9$ entity are well known [36]. Typically, such a metal triangle made

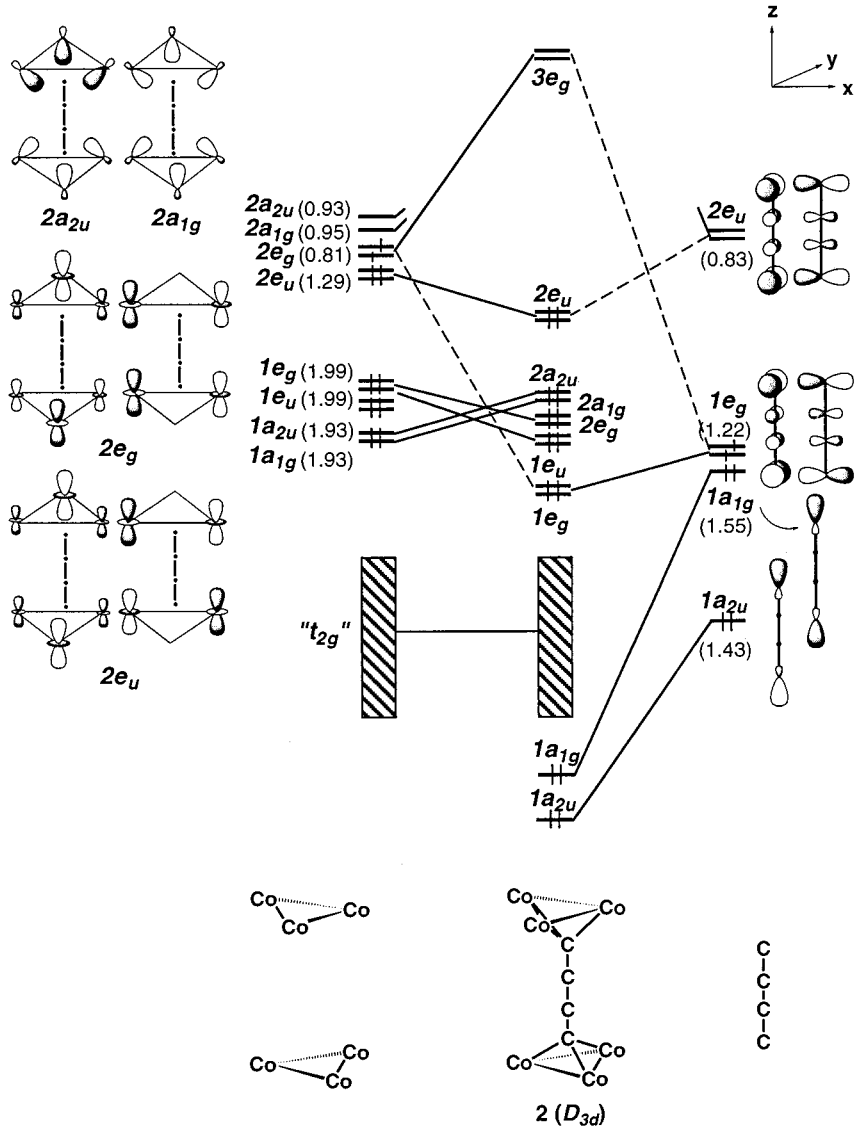

Fig. 3. Qualitative MO diagram based on EHT calculations for species **2** obtained from the interaction of the $\{(CO)_9Co_3\cdots Co_3(CO)_9\}$ fragment with the C_4 bridge. The low-lying FMO set of the metallic fragment is not drawn. Symmetry labels are given in D_{3d}. The numbers in brackets indicate the electron occupation of FMOs after interaction.

of three conical ML_3 groups gives rise to a nest of nine 't_{2g}' d-type levels below a low-lying set of three orbitals which extends predominantly in the metal plane and, at somewhat higher energy, a set of three orbitals extending mainly above the metal plane. Consequently, the $\{(CO)_9Co_3\cdots Co_3(CO)_9\}$ fragment exhibits two sets of six FMOs somewhat separated in energy ($1a_{1g}$, $1a_{2u}$, $1e_g$, $1e_u$) and ($2e_u$, $2e_g$, $2a_{1g}$ and $2a_{2u}$), lying above a 't_{2g}' block of 18 orbitals (see the left-hand side of Fig. 3). Among the sixteen MOs of the linear C–C≡C–C unit, only the six FMOs (the σ-type $1a_{2u}$ and $1a_{1g}$ and π-type $1e_g$ and $2e_u$ orbitals) that may be involved in interaction with the metallic fragment are shown on the right-hand side of Fig. 3. They are mainly localized on the C_α atoms (87, 73, 78, and 75% for $1a_{2u}$, $1a_{1g}$, $1e_g$, and $2e_u$, respectively).

When molecule **2** is built, the six lowest FMOs of the metallic fragment extending mainly in the metal planes hardly interact with the C_4 ligand and remain almost unperturbed after interaction (see their electron occupation in Fig. 3). They are occupied for the observed count of 96 MVEs, and are responsible for the six metal–metal bonding contacts. Indeed, the main bonding interactions between the two fragments occur between the upper metallic FMO set and the FMOs of the C_4 chain. For the count of 96 MVEs, the six M–C bonding combinations are occupied and well separated from the six M–C antibonding combinations which are vacant, ensuring the stability of cluster **2**.

It is expected that replacement of $Co(CO)_3$ groups in **2** by isolobal fragments would substantially modify the

Table 3
EH computed characteristics for different M_6C_4 cluster models

Compound	**2**	**2′**	**11-W**(*d*, *p*)[a]	**11-Mo**(*d*, *p*)[a]	**11-Mo**(*p*, *p*)[b]	**11-Mo**(*d*, *d*)[c]
	Binding energy (eV)					
	12.88	12.16	11.69	11.72	12.77	10.76
	HOMO/LUMO gap (eV)					
	2.26	2.20	1.51	1.55	1.65	1.45
	Atomic net charges					
Co	−0.09	−0.11	−0.32[d]/−0.08[e]	−0.31[d]/−0.06[e]	−0.06	−0.31
M		−0.42/−0.46	+1.40[d]/+1.31[e]	+1.24[d]/+1.14[e]	+1.15	+1.23
C_α	−0.26	−0.27/−0.29	−0.31[d]/−0.40[e]	−0.30[d]/−0.39[e]	−0.38	−0.30
C_β	−0.12	−0.13/−0.12	−0.16[d]/−0.17[e]	−0.15[d]/−0.16[e]	−0.15	−0.17
$[M_3L_n]$	+0.38	+0.39/+0.43	+0.51[d]/+0.53[e]	+0.48[d]/+0.51[e]	+0.53	+0.46
$[C_4]$	−0.75	−0.82	−1.04	−0.99	−1.06	−0.92
	C_4 FMO occupations					
$1e_u$ (π)	1.95/1.95	1.95/1.95	1.94/1.94	1.94/1.94	1.95/1.95	1.94/1.93
$1a_{2u}$ (σ_{nb})	1.43	1.44	1.46	1.46	1.46	1.45
$1a_{1g}$ (σ_{nb})	1.55	1.56	1.58	1.57	1.58	1.57
$1e_g$ (π_{nb})	1.22/1.22	1.23/1.23	1.22/1.34	1.22/1.32	1.23/1.35	1.21/1.29
$2e_u$ (π_{nb})	0.83/0.83	0.84/0.84	0.86/0.94	0.86/0.91	0.86/0.91	0.85/0.91
$2e_g(\pi^*)$	0.02/0.02	0.02/0.02	0.02/0.02	0.02/0.02	0.02/0.02	0.02/0.02
	Overlap populations					
Co–Co	0.19	0.19	0.16[d]/0.17[e]	0.17[d]/0.17[e]	0.17	0.17
Co–M	0.19/0.20	0.19[d]/0.11[e]	0.19[d]/0.11[e]	0.11	0.19	
Co–C_α	0.48	0.48	0.45[d]/0.45[e]	0.45[d]/0.45[e]	0.45	0.45
M–C_α		0.48	0.43[d]/0.55[e]	0.41[d]/0.53[e]	0.53	0.41
C_α–C_β	1.09	1.09	1.10[d]/1.10[e]	1.10[d]/1.10[e]	1.10	1.10
C_β–C_β	1.71	1.71	1.72	1.72	1.72	1.72

[a] *Distal/proximal* isomer (experimentally observed).
[b] *Proximal/proximal* isomer.
[c] *Distal/distal* isomer.
[d] *Distal.*
[e] *Proximal.*

extent of localization and energy of the metallic FMOs [37–39]. For instance, in $Co_2Mo(CO)_8Cp$ in which one $Co(CO)_3$ group of **2** is replaced by an $Mo(CO)_2Cp$ fragment, the localization of the higher FMO set of the heterometallic fragment is more heavily weighted towards the molybdenum atom than to its cobalt partners, compared to that in $Co_3(CO)_9$ [37,39]. Therefore, this must change the electronic character of the interactions of the metallic fragment with the capping C_4 ligand. EHT calculations were performed on species **2′**, **11-Mo** and **11-W** in order to try to quantify the change in the M–C and C–C bonding in the M_6C_4 clusters upon substitution of $Co(CO)_3$ by $Co(CO)_2(PH_3)$ or $MCp(CO)_2$ (M = Mo or W) units (geometries were idealized and M–M, M–C and C–C distances were kept constant to allow comparison, see Section 4 for the details of the calculations). The main results are collected in Table 3.

Replacement of $Co(CO)_3$ units by slightly more electron-rich $Co(CO)_2(PH_3)$ fragments hardly affects the electronic properties of the M_6C_4 complexes. Comparable results are obtained for **2** and $\{Co_3(CO)_8(PH_3)(\mu_3\text{-}C)\}C{\equiv}C\{(\mu_3\text{-}C)Co_3(CO)_7(PH_3)_2\}$ (**2′**) in which three $Co(CO)_3$ groups are replaced by three $Co(CO)_2(PH_3)$ groups (see Table 3). Starting from neutral fragments, a total donation of 0.745 electron occurs from the metallic fragment towards the carbon ligand in **2**. In **2′** 0.82 electron is transferred from the metallic fragment towards the C_4 bridge. Surprisingly enough, the additional electron density on the Co atoms tethered to phosphine ligands with respect to that of the Co atoms attached only to CO ligands (atomic net charge of ca. −0.45 vs. −0.11) is not transferred to the C_4 unit. Consequently the M–C and C–C bonding in species **2** and **2′** is nearly identical (see Table 3). Binding energies

between the metallic fragment and the C_4 bridge are comparable (12.88 vs. 12.11 eV) and HOMO–LUMO gaps are similar (2.26 vs. 2.20 eV).

Replacement of $Co(CO)_3$ units by $MCp(CO)_2$ units leads to some change in the M–M and M–C bonding but not in the C–C bonding with respect to that in **2** (see Table 3). The metallic core is less firmly bound to the C_4 unit in these substituted species observed in the solid state than in the hexacobalt species **2** and **2′**. The binding energy between the metallic moiety and the C_4 ligand is 11.69 and 11.72 eV for **11-W** and **11-Mo**, respectively (designated **11-W**(*d*, *p*) and **11-Mo**(*d*, *p*) in Table 3, see below) in comparison to 12.88 eV for **2**. The HOMO–LUMO gaps are somewhat smaller in **11-W** and **11-Mo** than in **2**.

Both compounds **11-Mo** and **11-W** crystallize with one Cp ligand oriented *distal* and the other *proximal* to the carbon chain (*distal*/*proximal* (*d*, *p*) isomeric forms). However, they are fluxional in solution meaning that they might interconvert into the other isomeric *proximal*/*proximal* (*p*, *p*) and *distal*/*distal* (*d*, *d*) arrangements (vide supra). EHT calculations were carried out on these (*p*, *p*) and (*d*, *d*) arrangements in the case of Mo. The results are compared to those of the observed (*d*, *p*) isomer **11-Mo** in Table 3 (comparable results are obtained in the case of **11-W**). Although not observed in the solid, the (*p*, *p*) form is computed to be the most stable arrangement. It is 0.96 and 1.93 eV more stable than the (*d*, *p*) and (*d*, *d*) forms, respectively (the idealized geometries were not optimized, see the details of the calculations in Section 4). It has been suggested from previous work on species containing the $MCo_2Cp(CO)_8(\mu_3\text{-}C–)$ (M = Mo or W) unit, that the *proximal* orientation of the $MCp(CO)_2$ fragment with respect to the carbon atom leads to significant electronic donation to the other two metal atoms and, presumably, to the carbon ligand [34,40,41]. This is not what we observed in compound **11-Mo**. Indeed, with the Cp ligand oriented in the *proximal* position, the metallic FMOs localized on the Mo centers point towards the position of the C_α atom, whereas in the *distal* orientation, they point rather away from C_α towards the Co atoms. Consequently the interaction between the metallic fragment and the C_4 bridge is stronger in the (*p*, *p*) isomer than in the (*d*, *d*) isomer. As reported in Table 3, the binding energy between the metallic and C_4 fragments is more important in the former than in the latter (12.77 vs. 10.76 eV). Note that the binding energy for the (*p*, *p*) form is close to that computed for **2**. That of the (*d*, *p*) isomer observed experimentally in the solid state is intermediate (11.72 eV). Stronger M_6–C_4 interactions lead to slightly larger HOMO–LUMO gaps (see Table 3).

Significant electron donation occurs from Mo to C_α in the (*p*, *p*) isomeric arrangement, enhancing the Mo–C bonds (the Mo–C_α overlap population is 0.53 compared to 0.41 in the (*d*, *d*) arrangement). In the (*d*, *d*) isomer, electron transfer occurs rather from Mo to Co leading to strong Co–Mo bonding. The Co–Mo overlap populations are 0.19 in the (*d*, *d*) isomer and 0.11 in the (*p*, *p*) isomer. The energy gain in Co–M bonding in the (*d*, *d*) isomer with respect to that in the (*p*, *p*) isomer is not sufficient to overcome the energy gain of M–C bonding in the (*p*, *p*) isomer with respect to that in the (*d*, *d*) isomer. As said earlier, the (*d*, *d*) arrangement is less stable than the (*p*, *p*) arrangement. Results obtained for the *distal* and *proximal* cluster parts of the (*d*, *p*) isomer are similar to those of the (*d*, *d*) and (*p*, *p*) isomers, respectively. Such results computed on idealized geometries are in agreement with the Co–M and M–C distances measured experimentally in **11-Mo**, **11-W**, and **12** (see Table 1). The M–M separations are shorter in the Co_2M_{distal} part than in the $Co_2M_{proximal}$ part. On the other hand, the M–C_α (M = Mo, W) distance is longer in the cluster moiety bearing the *distal* Cp ligand than in the cluster moiety bearing the *proximal* Cp ligand.

These results lead us to conclude that the (*d*, *p*) arrangement of compounds **11-Mo** and **11-W** observed in the solid state is rather due to crystal packing forces which must counterbalance the diminution of the bonding energy between the metallic and C_4 fragments with respect to that in the most electronically stable (*p*, *p*) form. Contrary to what one may think at first sight, however, the respective charges of each M_3L_n cluster moiety do not differ sufficiently to induce a dipole moment in the molecule (see Table 3).

The C_4 bridge is more negatively charged in model **11** than in compounds **2** and **2′** (see Table 3). However, this hardly affects the C–C bonding in these species. The C_α–C_β and C_β–$C_{\beta'}$ overlap populations are identical in all models (ca. 1.10 and 1.72, respectively) and comparable to those computed for a 'saturated' $(C_4)^{6-}$ 2-butynido ligand (1.01 and 1.67, respectively). Indeed, the increase of electron density on the carbon chain in the former complexes with respect to the latter complexes occurs mainly on the C_α atoms (the charges borne by the C_β atoms are similar in all models) and is due to a more important electron occupation of the C_4 FMOs after interaction with the metallic fragment. These FMOs are mainly localized on the C_α atoms and are C–C nonbonding overall (see Fig. 2). Consequently, their occupation slightly differs according to the model considered, but almost does not perturb the C–C separations. Although at first sight the C_α–C_β and C_β–$C_{\beta'}$ distances found experimentally in **2** and **2′** are slightly shorter and longer, respectively [8,9], they are not accurate enough to be differentiated from the corresponding distances in complexes **11** and **12**.

Delocalization between the metallic caps via the carbon chain would occur if the low-lying σ and π orbitals and high-lying σ^* and π^* orbitals localized on the

central C atoms of the C_4 chain were involved in the M_6–C_4 bonding. Our calculations indicate that the π* FMOs localized on the central C–C bond are not involved in the M_6–C_4 interaction, so that the degree of electronic delocalization between the metallic cores through the C_4 bridge is very weak. For instance, the occupation of the low-lying π $1e_u$ and high-lying π* $2e_g$ orbitals (not shown in Fig. 2) which are strongly localized on the C_β atoms (75 and 78%, respectively) is close to two and zero, respectively, after interaction with the metallic fragment (see Table 3). Comparison of the results obtained for the model **11-Mo**(*d*, *p*) to those obtained for the other isomeric (*d*, *d*) and (*p*, *p*) arrangements gives additional evidence of the localized bonding character between the $M_3(\mu_3\text{-C})$ units and the central C≡C bond of the carbon chain. In other words, there is hardly any communication between the two metallic moieties through the C_4 bridge in such species. These M_6C_4 species are best considered as permetalated 2-butyne molecules.

Electrochemical studies have shown that the hexacobalt compounds **2** and **2′** undergo two reversible one-electron reduction processes which, according to the authors, is indicative of a moderate electronic interaction between the two redox metallic caps [9,41]. Clusters M_6C_4 have orbitals in the LUMO region such as $3e_g$ in Fig. 2, which are M–C_α antibonding and not too high in energy, conferring some tunable electron-acceptor character to these species. Therefore, we think that small changes in geometry involving metallic triangles and/or the C_4 bridge must occur upon reduction which may cause some communication via the carbon chain, which is not observed in the case of neutral species [42]. As mentioned earlier, HOMO–LUMO gaps computed for **11-Mo** and **11-W** species are considerably smaller than those computed for species **2** and **2′**. Such heterometallic M_6C_4 compounds should be more easily electrochemically reduced. On the other hand, they must be difficult to oxidize, in contrast to the diyndiyl bimetallic complexes such as $\{Ru(PPh_3)_2Cp\}_2(\mu\text{-}C_4)$ [27]. Despite the fact that both species contain a linear C_4 chain linking two metallic caps, their electronic structures and consequently their electronic behaviour, are quite different. The HOMOs in M_6C_4 are rather low in energy and strongly M–C bonding. Electron depopulation would lead to some partial (or total) bond breaking between the C_4 bridge and the trimetallic moieties. In constrast, HOMOs in the M_2C_4 complexes are M–C antibonding and rather high in energy, whereas the LUMOs are very high in energy and mainly C–C π* antibonding [43–45]. Partial (or total) depopulation of the HOMOs is possible leading to multiply oxidized species [27]. In conclusion, M_6C_4 and M_2C_4 compounds in which the carbon termini are bound to three and one metal atoms, respectively, belong to different classes of carbon-chain containing complexes.

2.3. Reaction of **9-W** with $Co_2(\mu\text{-dppm})(CO)_6$

The reaction between **9-W** and $Co_2(\mu\text{-dppm})(CO)_6$ proceeded smoothly in refluxing benzene to give $Co_2\{\mu\text{-}[Cp(OC)_3W]C_2C{\equiv}C[W(CO)_3Cp]\}(\mu\text{-dppm})(CO)_4$ (**13**) in good yield (72%). The ^1H resonances for the methylene portion of the dppm ligand were found at δ 3.43 and 3.86, and two distinct Cp signals were found at δ 5.52 and 5.87. In the ^{13}C-NMR spectrum, two Cp resonances at δ 91.81 and 95.62 were present, but only two of the expected four signals for the C_4 chain appeared, at δ 109.50 and 76.28. The positive-ion ES-MS of **13** as a methanolic solution containing NaOMe gave both $[M + Na]^+$ and $[M + H]^+$ ions. Other spectroscopic and microanalytical data were in accord with the proposed structure.

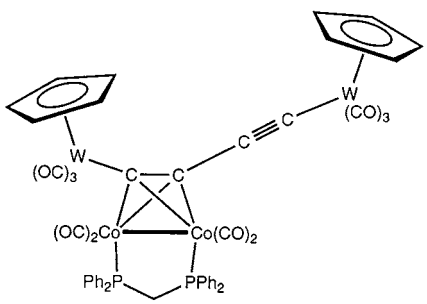

(13)

The formation of the simple adduct **13** from the reaction of the bulkier $Co_2(\mu\text{-dppm})(CO)_6$ reagent with **9-W** may seem to contradict the steric argument used to explain the formation of **7** from **5** and $Co_2(CO)_8$. However, the isolation of **13** may simply indicate that the dppm ligand prevents the W centre from approaching the Co_2 unit. This implies that the formation of the new metal–metal bonds required to give the $Co_2M(\mu_3\text{-CR})$ fragment is the driving force behind the formation of clusters **11** and **12**.

3. Conclusion

The results described above are consistent with one of the C≡C triple bonds in complexes $W(C{\equiv}CC{\equiv}CR)(CO)_3Cp$ readily coordinating a $Co_2(CO)_6$ fragment if the R group is small enough to allow it to be accommodated. NMR evidence points to the group, i.e. the least sterically hindered one, being the site of coordination. However, when R = (Mo/W)$(CO)_3$Cp, further interaction between the two metal carbonyl groups results in CO expulsion and cluster formation. In the course of this reaction, formal oxidation of the C_4 chain to the dicarbyne ligand occurs. Further studies of these unique reactions are under way.

4. Experimental

4.1. General reaction conditions

All reactions were carried out under standard Schlenk conditions using a double manifold N_2-vacuum line. Solvents were dried and distilled prior to use according to convention. Elemental analyses were by the Canadian Microanalytical Service, Delta, B.C. Preparative TLC was carried out on glass plates (20 × 20 cm) coated with silica gel (Merck 60 GF_{254}, 0.5 mm thick).

4.2. Reagents

The compounds M(C≡CC≡CH)(CO)$_3$Cp (M = W **5-W**, Mo **5-Mo**) [16,17], {Cp(OC)$_2$Fe}C≡CC≡C{W(CO)$_3$Cp} (**7**) [16], {Cp(OC)$_3$M}C≡CC≡C{M′(CO)$_3$Cp} (M = M′ = W **9-W**, Mo **9-Mo**; M = W, M′ = Mo **10**) [16] and Co_2(μ-dppm)(CO)$_6$ [46] were synthesised by the literature methods. $Co_2(CO)_8$ (Strem) was used as received.

4.3. Spectroscopy

IR spectra were recorded on a Perkin Elmer 1700X FT-IR spectrometer using 0.5 mm pathlength solution cells fitted with NaCl windows. NMR spectra were recorded on a Bruker ACP300 (^{1}H at 300.13 MHz, ^{13}C at 75.47 MHz) or Varian Gemini 200 (^{1}H at 199.98 MHz, ^{13}C at 50.29 MHz) instruments in $CDCl_3$. Electrospray mass spectra (ES-MS) were obtained using a VG Platform II mass spectrometer with a 10 μl injection loop. Samples were examined over a range of cone voltages (20–90 V) to give optimal spectra; in some cases, spectra of solutions containing NaOMe were also recorded [47].

4.3.1. Co_2{μ-HC_2C≡C[W(CO)$_3$Cp]}(CO)$_6$ (**6-W**)

A solution of W(C≡CC≡CH)(CO)$_3$Cp (150 mg, 0.39 mmol) in benzene (15 ml) was treated with $Co_2(CO)_8$ (135 mg, 0.40 mmol) in several portions over 15 min. The solvent was removed from the resulting red–brown solution and the residue purified by preparative TLC (light petroleum/acetone, 4/1). Crystallisation of the only significant band (CH_2Cl_2) gave deep red Co_2{μ-HC_2C≡C[W(CO)$_3$Cp]}(CO)$_6$ (**6-W**) (100 mg, 38%). Anal. Found: C, 32.49; H, 1.00%. Anal. Calc. $C_{18}H_6O_9Co_2W$: C, 32.36; H, 0.90%. IR (cyclohexane, cm^{-1}): ν(C≡C) 2091 m; ν(CO) 2054 vs, 2039 s, 2024 vs, 1965 vs, 1954 s cm^{-1}. ^{1}H-NMR ($CDCl_3$): δ_H 6.04 (s, 1H, C_2H), 5.67 (s, 5H, Cp). ^{13}C-NMR δ_C 227.70 (s, WCO), 210.15 (s/d, J_{CW}183 = 128 Hz, WCO), 199.66 (br, CoCO), 123.13 (s, C_α), 94.34 (s, C_β), 91.70 (s, Cp), 73.84 (s, C_γ), 71.56 (s, C_δ). FAB-MS (m/z): 668, M$^+$; 640–528 [M-nCO]$^+$ (n = 1–5).

4.3.2. Co_2{μ-HC_2C≡C[Mo(CO)$_3$Cp]}(CO)$_6$ (**6-Mo**)

The analogous reaction between Mo(C≡CC≡CH)-(CO)$_3$Cp (150 mg, 0.51 mmol) and $Co_2(CO)_8$ (175 mg, 0.51 mmol) gave Co_2{μ-HC_2C≡C[Mo(CO)$_3$Cp]}(CO)$_6$ (**6-Mo**) (113 mg, 40%) from cyclohexane. Anal. Found: C, 37.56; H, 1.15%. Anal. Calc. $C_{18}H_6O_9Co_2Mo$: C, 37.25; H 1.03%. IR (cyclohexane): ν(C≡C) 2091 m; ν(CO) 2054 vs, 2044 vs, 2029 vs, 2024 vs, 1977 vs, 1967 s cm^{-1}. ^{1}H-NMR ($CDCl_3$): δ_H 6.06 (s, 1H, C_2H), 5.57 (s, 5H, Cp). ^{13}C-NMR: δ_C 237.63 (s, MoCO), 221.22 (s, MoCO), 199.64 (br, CoCO), 123.43 (s, C_α), 109.52 (s, C_β), 93.11 (s, Cp), 74.07 (s, C_γ), 71.35 (s, C_δ). FAB-MS (m/z): 526–330, [M-nCO]$^+$ (n = 2–9).

4.3.3. Co_2{μ-[Cp(OC)$_2$Fe]C_2C≡C[W(CO)$_3$Cp]}(CO)$_6$ (**8**)

This complex was prepared similarly from {Cp(OC)$_2$Fe}C≡CC≡C{W(CO)$_3$Cp} (100 mg, 0.18 mmol) and $Co_2(CO)_8$ (62 mg, 0.18 mmol) and isolated as a hemi-CH_2Cl_2 solvate following preparative TLC and crystallisation (CH_2Cl_2/hexane) (102 mg, 64%). Anal. Found: C, 34.45; H 1.29%. Anal. Calc. $C_{25}H_{10}O_{11}Co_2FeW.0.5CH_2Cl_2$: C, 34.55; H, 1.25%. IR (cyclohexane): ν(CO) 2076 s, 2039 vs, 2009 s, 2004 (sh), 1986 m, 1960 s, 1950 s cm^{-1}. ^{1}H-NMR ($CDCl_3$): δ_H 5.67 (s, 5H, WCp), 5.32 (s, 1H, 0.5CH_2Cl_2), 5.17 (s, 5H, FeCp). ^{13}C-NMR: δ_C 228.97 (s, WCO), 213.41 (s, WCO), 210.41 (s, FeCO), 201.66 (br, CoCO), 125.79 (br, C_α), 106.09 (s, C_β), 97.86 (s, C_γ), 91.85 (s, WCp), 86.68 (s, FeCp), 85.68 (s, C_δ). FAB-MS (m/z): 844, M$^+$; 816–592, [M-nCO]$^+$ (n = 1–9).

4.3.4. {Cp(OC)$_8Co_2M(\mu_3$-C)}C≡C{(μ_3-C)Co_2M′(CO)$_8$-Cp} (M = M′ = W, **11-W**; Mo, **11-Mo**; M = W, M′ = Mo, **12**)

A rapidly stirred suspension of {W(CO)$_3$Cp}$_2$(μ-C_4) (100 mg, 0.14 mmol) in benzene (15 ml) was treated with $Co_2(CO)_8$ (96 mg, 0.28 mmol) in one portion and stirred until the suspension had dissolved. The resulting red–brown solution was filtered and the filtrate purified by TLC (light petroleum/acetone, 4/1). The only significant band (R_f 0.3) was crystallised (CH_2Cl_2/hexane) to give deep red blocks of {Cp(CO)$_8Co_2W(\mu_3$-C)}$_2C_2$ (**11-W**) (66 mg, 38%).

The complexes **11-Mo** (M = M′ = Mo, 40%) and **12** (M = W, M′ = Mo, 19%) were prepared in identical manner from the reactions of **9-Mo** (100 mg, 0.18 mmol) or **10** (150 mg, 0.24 mmol) with a two-fold excess of $Co_2(CO)_8$.

4.3.5. Complex **11-W**

Anal. Found: C, 28.99; H, 0.80%. Anal. Calc. $C_{30}H_{10}O_{16}Co_4W_2$: C, 29.29; H, 0.81%. IR (cyclohexane): ν(CO) 2077 m, 2064 m, 2040 vs, 2030 s, 2014 m, 2003 m, 1994 m, 1944 m, 1984 (sh), 1961 s, 1951 s, 1891 s cm^{-1}. ^{1}H-NMR ($CDCl_3$): δ_H 5.56 (s, Cp). ^{13}C-NMR:

Table 4
Crystal data and refinement details for complexes **11-W, 11-Mo** and **12**

Compound	**11-Mo**	**11-W**	**12**
Emperical formula	$C_{30}H_{10}Co_4Mo_2O_{16}$	$C_{30}H_{10}Co_4O_{16}W_2$	$C_{30}H_{10}Co_4MoO_{16}W$
Formula weight	1054.0	1229.8	1141.9
Crystal system	Monoclinic	Monoclinic	Monoclinic
Space group	$P2_1/c$	$P2_1/c$	$P2_1/c$
a (Å)	16.061(2)	16.035(6)	16.041(3)
b (Å)	12.223(3)	12.190(3)	12.205(4)
c (Å)	20.621(3)	20.623(6)(5)	20.609(4)
β (°)	120.17(1)	120.08(2)	120.12(2)
V (Å^3)	3500	3488	3490
Z	4	4	4
$D_{calc.}$ (g cm^{-3})	2.000	2.342	2.173
$F(000)$	2040	2296	2168
Crystal size (mm)	$0.45\times0.45\times0.65$	$0.22\times0.33\times0.48$	$0.28\times0.38\times0.19$
A^* (min., max.)	2.36, 2.92 (gaussian)	3.59, 9.52 (analytical)	1.90, 2.84 (analytical)
μ (cm^{-1})	26.2	85.2	55.6
$2\theta_{max}$ (°)	60	60	55
N	10185	10474	7984
N_0	7756	6736	5519
R	0.043	0.050	0.033
R_w	0.050	0.052	0.033

δ_C 202.96 (br, CO), 126.48 (s, C≡C), 91.32 (s, Cp). ES-MS (after addition of NaOMe) (m/z): 1259, [M + OMe]$^-$.

4.3.6. Complex *11-Mo*

Anal. Found: C, 33.42; H, 0.90%. Anal. Calc. $C_{30}H_{10}O_{16}Co_4Mo_2$: C, 34.15; H, 0.95%. IR (cyclohexane): ν(CO) 2085 m, 2074 m, 2064 m, 2044 vs, 2038 s, 2014 m, 2005 s, 1993 m, 1975 s, 1964 s, 1954 (sh), 1897 s cm^{-1}. ^{1}H-NMR ($CDCl_3$): δ_H 5.49 (s, Cp). ^{13}C-NMR: δ_C 269.85 (s, μ_3-C), 207.90 (br, CO), 125.94 (s, C≡C), 93.45 (s, Cp). ES-MS (with NaOMe) (m/z): 1084, [M + OMe]$^-$.

4.3.7. Complex *12*

Anal. Found: C, 31.40; H, 0.89%. Anal. Calc. $C_{30}H_{10}O_{16}Co_4MoW$: C, 31.52; H, 0.88%. IR (cyclohexane): ν(CO) 2085 m, 2074 s, 2066 m, 2047 vs, 2037 m, 2025 s, 2004 s, 1941 (br), 1894 s (br) cm^{-1}. ^{1}H-NMR ($CDCl_3$): δ_H 5.57 (s, 5H, WCp), 5.49 (s, 5H, MoCp). ^{13}C-NMR: δ_C 207.92, 202.85 (2 × br, CO), 127.65 (s, Co_2MoCC), 124.76 (s, Co_2WCC), 93.56 (s, MoCp), 91.21 (s, WCp). ES-MS (with NaOMe) (m/z): 1173, [M + OMe]$^-$.

4.3.8. Co_2(μ-dppm){μ-[Cp(OC)$_3$W]C_2C≡C{W(CO)$_3$-Cp]}(CO)$_4$ (*13*)

A suspension of {W(CO)$_3$Cp}$_2$(μ-C$_4$) (100 mg, 0.14 mmol) in benzene (15 ml) was treated with Co_2(μ-dppm)(CO)$_6$ (190 mg, 0.28 mmol) and warmed in an oil bath at 80°C for 4 h. The suspension dissolved over this time to give a red–brown solution. Removal of the solvent followed by preparative TLC (light petroleum/acetone, 7/3) gave a single dark purple band from which red crystals of Co_2(μ-dppm){μ-[Cp(OC)$_3$W]-C_2C≡C[W(CO)$_3$Cp]}(CO)$_4$ (**13**) (134 mg, 69%) were obtained ($CHCl_3$/MeOH). Anal. Found: C, 43.14; H 2.81%. Anal. Calc. $C_{49}H_{32}O_{10}P_2Co_2W_2\cdot0.5CHCl_3$: C, 42.84; H 2.36%. IR (cyclohexane): ν(CO) 2039 m, 2027 m, 2000 m, 1986 s, 1956 vs, 1939 vs, 1923 (sh) cm^{-1}. ^{1}H-NMR ($CDCl_3$): δ_H 7.51–7.08 (m, 20H, Ph), 5.87, 5.52 (2 × s, 2 × 5H, 2 × Cp), 3.86, 3.43 (2 × dt, J_{HH} = 12 Hz, J_{PH} = 11 Hz, CH_2P_2). 13C-NMR: δ_C 212.58 (t, J_{WC} = 3Hz, WCO), 210.69 (s, WCO), 204.41 (br, CoCO), 139.29–127.67 (m, PPh), 109.50 (br, C$_\alpha$), 95.62, 91.81 (2 × s, 2 × Cp), 76.28 (s, C$_\beta$), 33.72 (t, J_{PC} = 20 Hz, CH_2P_2. ES-MS (m/z) (with NaOMe): 1351, [M + Na]$^+$; 1328, M].

4.4. Crystallography

Unique room temperature diffractometer data sets were recorded (monochromatic Mo–Kα radiation, λ = 0.7107$_3$ Å; T = 295 K) and used in the full matrix least squares refinements after absorption correction. Anisotropic thermal parameter forms were refined; $(x, y, z, U_{iso})_H$ were included constrained at estimated values. Phenyl rings were refined as rigid bodies. Conventional residuals R, R_w on $|F|$ at convergence are given, statistical weights derivative of $\sigma^2(I) = \sigma^2(I_{diff}) = 0.0004\sigma^4(I_{diff})$ being employed. Neutral atom complex scattering factors were employed, computation using the XTAL 3.4 program system [48] implemented by Hall et al. Pertinent results are given in Fig. 1 and Tables 1 and 4; material deposited comprises all coordinates and thermal parameters, full molecular non-hydrogen geometries and structure factor amplitudes.

4.4.1. Theoretical calculations

4.4.1.1. Extended Hückel Theory calculations. Extended Hückel calculations were carried out within the extended Hückel formalism [49,50] using the program CACAO [51]. The exponents (ζ) and the valence shell ionization potentials (H_{ii} in eV) were respectively: 1.3, −13.6 for H 1s; 1.625, −21.4 for C 2s; 1.625, −11.4 for C 2p; 2.275, −32.4 for O 2s; 2.275, −14.8 for O 2p; 1.6, −18.6 for P 3s; 1.6, −14.0 for P 3p; 2.00, −9.21 for Co 4s; 2.00, −5.29 for Co 4p; 1.956, −8.34 for Mo 5s; 1.921, −5.24 for Mo 5p; 2.341, −8.26 for W 6s; 2.309, −5.17 for W 6p. The H_{ii} value for Co 3d, Mo 4d, and W 5d was at −13.18, −10.50, and −10.37, respectively. A linear combination of two Slater-type orbitals with exponents $\zeta_1 = 5.55$ and $\zeta_2 = 1.90$; $\zeta_1 = 4.54$ and $\zeta_2 = 1.90$; $\zeta_1 = 4.982$ and $\zeta_2 = 2.068$ with the weighting coefficients $c_1 = 0.5551$ and $c_2 = 0.6461$; $c_1 = 0.5899$ and $c_2 = 0.5899$; $c_1 = 0.694$ and $c_2 = 0.5631$ were used to represent the Co 3d, Mo 4d, and W 5d atomic orbitals, respectively. The different molecular models used were idealized based on the experimental structure of **2**. The following bond distances (Å) and bond angles (°) were used: Co–Co = 2.47; Co–Mo = 2.70; Co–W = 2.70; Co–C_α = 1.92; Mo–C_α = 2.09; W–C_α = 2.09; Co–P = 2.15; Co–C_{eq}(O) = 1.78; Co–C_{ax}(O) = 1.82; Mo–C(Cp) = 2.32; W–C(Cp) = 2.32; Mo–C(0) = 1.98; W–C(0) = 1.98; C_α–C_β = 1.371; C_β–$C_{\beta'}$ = 1.241; C–O = 1.14; P–H = 1.42; C_α–C_β–$C_{\beta'}$ = 180. Co–Co, Co–C, and C–C distances were kept constant in all computed models to allow comparison. Comparable results were obtained using the experimental structures.

4.4.1.2. Density Functional Theory calculations. Density Functional calculations were carried out on cluster **2** using the Amsterdam Density Functional (ADF) program [52] developed by Baerends and coworkers [53–56] using the local density approximation (LDA) in the Vosko–Wilk–Nusair parametrization [57]. The atom electronic configurations were described by a double-ζ Slater-type orbital (STO) basis set for H 1s, C 2s and 2p, O 2s and 2p, P 3s and 3p, augmented with a 3d single-ζ polarization function for the carbon atoms of the C_4 chain. A triple-ζ STO basis set was used for Co 3s, 3p, 3d and 4s, augmented with a single-ζ 4p polarization function. A frozen-core approximation was used to treat the 1s core shell of C and O, and the 1s, 2s, 2p core shells of Co [53]. The geometry was optimized using the analytical gradient method implemented by Verluis and Ziegler [58].

Acknowledgements

Support of this work by the Australian Research Council is gratefully acknowledged. P.J. Low was the holder of an Australian post-graduate award. We thank Professor Brian Nicholson (University of Waikato, Hamilton, New Zealand) for the elctrospray mass spectra. J.-F. Halet thanks the University of Adelaide and the CNRS for his stay at Adelaide in August 1997. S. Kahlal and J.-F. Halet thank the Centre de Ressources Informatiques (CRI) of Rennes and the Institut de Développement et de Ressources en Informatique Scientifique (IDRIS-CNRS) of Orsay (project 970649) for computing facilities.

References

[1] K. Sonogashira, S. Kataoka, S. Takagashi, N. Hagihara, J. Organomet. Chem. 160 (1978) 319.
[2] A. Wong, P.C.W. Kang, C.D. Tagge, D.R. Leon, Organometallics 9 (1990) 1992.
[3] N. Le Narvor, C. Lapinte, J. Am. Chem. Soc. 117 (1995) 7129.
[4] S.B. Falloon, W. Weng, A.M. Arif, J.A. Gladysz, Organometallics 16 (1997) 2008.
[5] M. Akita, M.-C. Chung, A. Sakurai, S. Sugimoto, M. Terada, M. Tanaka, Y. Moro-oka, Organometallics 16 (1997) 4882.
[6] J. Gil-Rubio, M. Laubender, H. Werner, Organometallics 17 (1998) 1202.
[7] D.M. Norton, C.L. Stern, D.F. Shriver, Inorg. Chem. 33 (1994) 2701.
[8] R.J. Dellaca, B.R. Penfold, B.H. Robinson, W.T. Robinson, J.L. Spencer, Inorg. Chem. 9 (1970) 2204.
[9] G. H. Worth, B. H. Robinson, J. Simpson, Organometallics 11 (1992) 3863.
[10] C.J. Adams, M.I. Bruce, E. Horn, B.W. Skelton, E.R.T. Tiekink, A.H. White, J. Chem. Soc. Dalton Trans. (1993) 3299.
[11] M.I. Bruce, B.W. Skelton, A.H. White, N.N. Zaitseva, J. Chem. Soc. Dalton Trans. (1996) 3151.
[12] S.B. Falloon, A.M. Arif, J.A. Gladysz, Chem. Commun. (1997) 629.
[13] C.J. Adams, M.I. Bruce, B.W. Skelton, A.H. White, J. Organomet. Chem. 450 (1993) C9.
[14] P. Blenkiron, G.D. Enright, P.J. Low, J.F. Corrigan, N.J. Taylor, Y. Chi, J.-Y. Saillard, A.J. Carty, Organometallics 17 (1998) 2447.
[15] M.I Bruce, P. Hinterding, E.R.T. Tiekink, B.W. Skelton, A.H. White, J. Organomet. Chem. 450 (1993) 209.
[16] M.I. Bruce, M. Ke, P.J. Low, Chem. Commun. (1996) 2405.
[17] M.I. Bruce, M. Ke, P.J. Low, B.W. Skelton, A.H. White, Organometallics 17 (1998) 3539.
[18] G.A. Carriedo, V. Riera, D. Miguel, J. Organomet. Chem. 342 (1988) 373.
[19] K. Yasufuku, H. Yamazaki, Bull. Chem. Soc. Jpn. 45 (1972) 2664.
[20] M.I. Bruce, D.N. Duffy, M.G. Humphrey, Aust. J. Chem. 39 (1986) 159.
[21] W. Bernhardt, H. Vahrenkamp, Organometallics 5 (1986) 2388.
[22] W. Hübel, R. Merenyi, Chem. Ber. 96 (1963) 930.
[23] G. Peyronel, A. Ragini, E.F. Trogu, Gazz. Chim. Ital. 97 (1967) 1327.
[24] R.S. Dickson, G.R. Tailby, Aust. J. Chem. 22 (1969) 1143.
[25] K.H. Pannell, G.M. Crawford, J. Coord. Chem. 2 (1973) 251.
[26] R.S. Dickson, P.J. Fraser, Adv. Organomet. Chem. 12 (1974) 323.
[27] M.I. Bruce, P.J. Low, L. Denisovich, S. Perugudova, N.A. Ustynyuk, Mendeleev Commun. (1996) 200.
[28] F.G.A. Stone, Angew. Chem. 96 (1984) 85; Angew. Chem. Int. Ed. Engl. 23 (1984) 89.

[29] Y. Chi, D.-K. Hwang, in: E.W. Abel, F.G.A. Stone, G. Wilkinson (Eds.), Comprehensive Organometallic Chemistry II, vol. 10, Pergamon, Oxford, 1995, p. 110.
[30] H. Beurich, H. Vahrenkamp, Chem. Ber. 115 (1982) 2385.
[31] M.J. Chetcuti, P.A.M. Chetuti, J.C. Jeffery, R.M. Mills, P.Mitrprachachon, S.J. Pickering, F.G.A. Stone, P. Woodward, J. Chem. Soc. Dalton Trans. (1982) 699.
[32] K.A. Sutin, L. Li, C.S. Frampton, B.G. Sayer, M.J. McGlinchey, Organometallics 10 (1991) 2362.
[33] M. Chetcuti, M. Green, J.A.K. Howard, J.C. Jeffery, R.M. Mills, G.N. Pain, S.J. Porter, F.G.A. Stone, A.A. Wilson, P. Woodward, J. Chem. Soc. Chem. Commun. (1980) 1057.
[34] H. Shimomura, X. Lei, M. Shang, T.P. Fehlner, Organometallics 16 (1997) 5302.
[35] D.M.P. Mingos, D.J. Wales, Introduction to Cluster Chemistry, Prentice-Hall, Englewood Cliffs, NJ, 1990.
[36] B.E.R. Schilling, R. Hoffmann, J. Am. Chem. Soc. 101 (1979) 3456.
[37] J.-F. Halet, J-Y. Saillard, R. Lissillour, M. J. McGlinchey, G. Jaouen, Inorg. Chem. 24 (1985) 218.
[38] J.-F. Halet, Coord. Chem. Rev. 143 (1995) 637.
[39] M.J. McGlinchey, in: M. Gielen (Ed.), Topics in Physical Organometallic Chemistry, vol. 4, Freund, London, 1992, p. 41.
[40] K.A. Sutin, L. Li, C.S. Frampton, B.G. Sayer, M.J. McGlinchey, Organometallics 10 (1991) 2362.
[41] D. Osella, O. Bambino, C. Nevi, M. Ravera, D. Bertolino, Inorg. Chim. Acta 206 (1993) 155.
[42] S. Kahlal, J.-F. Halet, unpublished results.
[43] M. Brady, W. Weng, Y. Zhou, J. W. Seyler, A.J. Amoroso, A.M. Arif, M. Böhme, G. Frenking, J.A. Gladysz, J. Am. Chem. Soc. 119 (1997) 775.
[44] P. Belanzoni, N. Re, A. Sgamellotti, C. Floriani, J. Chem. Soc. Dalton Trans. (1998) 1825.
[45] M.I. Bruce, K. Costuas, J.-F. Halet, P.J. Low, unpublished results.
[46] L.S. Chia, W.R. Cullen, Inorg. Chem. 14 (1975) 482.
[47] W. Henderson, J.S. McIndoe, B.K. Nicholson, P.J. Dyson, J. Chem. Soc. Dalton Trans. (1998) 519.
[48] S.R. Hall, G.S.D. King, J.M. Stewart (Eds.), The XTAL 3.4 Users' Manual, University of Western Australia, Lamb, Perth, 1994.
[49] R. Hoffmann, J. Chem. Phys. 39 (1963) 1397.
[50] R. Hoffmann, W.N. Lipscomb, J. Chem. Phys. 36 (1962) 2179.
[51] C. Mealli, D. Proserpio, J. Chem. Educ. 67 (1990) 399.
[52] Amsterdam Density Functional (ADF) Program, Release 2.0.1, Vrije Universteit, Amsterdam, Netherlands, 1996.
[53] E.J. Baerends, D.E. Ellis, P. Ros, Chem. Phys. 2 (1973) 41.
[54] E.J. Baerends, P. Ros, Int. J. Quantum Chem. S12 (1978) 169.
[55] P.M. Boerrigter, G. te Velde, E.J. Baerends, Int. J. Quantum Chem. 33 (1988) 87.
[56] G. te Velde, E.J. Baerends, J. Comput. Phys. 99 (1992) 84.
[57] S.D. Vosko, L. Wilk, M. Nusair, Can. J. Chem. 58 (1990) 1200.
[58] L. Verluis, T. Ziegler, J. Chem. Phys. 322 (1988) 88.